JOURNAL OF CATALYSIS 128, 248–263 (1991)

Synthesis and Characterization of New VPO Catalysts for Partial *n*-Butane Oxidation to Maleic Anhydride

N. HARROUCH BATIS,* H. BATIS,* A. GHORBEL,† J. C. VEDRINE,†
AND J. C. VOLTA†,[1]

*Laboratoire de Catalyse et Matériaux, Département de Chimie, Faculté des Sciences, Tunis, Tunisia; and
†Institut de Recherches sur la Catalyse, C.N.R.S., 2 Avenue A. Einstein, 69626 Villeurbanne Cedex, France

Received May 21, 1990; revised August 30, 1990

In order to try to control the V^{4+}/V^{5+} ratio of VPO catalysts for butane oxidation to maleic anhydride, a new method of preparation of these catalysts has been developed: it consists of the reaction of VCl_3 (V^{3+}) with V_2O_5 (V^{5+}) for the preparation of the precursor. Two series of catalysts have been prepared in aqueous and organic media. The V^{3+}/V^{5+} ratio has been varied and its influence on the physicochemical features and on the catalytic properties of the catalysts has been studied. The best catalysts in both preparation media correspond to $V^{3+}/V^{5+} = 1$ in the starting material. Catalysts have been characterized using X-ray diffraction, infrared spectroscopy, UV diffuse reflectance, Raman spectroscopy, ^{31}P MAS NMR, and XPS techniques. The combination of all these techniques led us to conclude that the best catalyst consisted of an oxidized surface (γ-$VOPO_4$) (V^{5+}) in interaction with reduced matrix ($(VO)_2P_2O_7$) (V^{4+}).

INTRODUCTION

Phosphorus–vanadium mixed oxide (VPO) is a unique catalyst possessing a surprisingly high selectivity in the oxidation of *n*-butane to maleic anhydride (MA) (*1–3*). For this reason, increasing attention has been paid to improving and better understanding the catalytic action of VPO catalysts.

It is established that the catalytic behavior of the VPO system depends on several factors: (i) preparation conditions, namely P/V atomic ratio in the starting mixture and aqueous or organic media, which leads to the obtention of the $VOHPO_4$, 0.5 H_2O precursor, (ii) activation conditions, i.e., conditions of pretreatment of the precursor, and (iii) catalytic conditions (*4–7*). These have attracted wide patent coverage and received a good deal of attention in the literature over the past decade (*2–4, 8, 9*).

The preparation of the precursor of these catalysts can be summarized in two procedures: (i) in an aqueous medium by V_2O_5 reduction with HCl (*5–7, 10*) or NH_4VO_3 reduction with oxalic or lactic acid (*8, 11–13*) followed by the addition of 85% H_3PO_4 and (ii) in an organic medium by V_2O_5 reduction with pure organic alcohols, isobutyl or isopropyl alcohols, or a mixture of alcohols (*6, 7, 10, 14*) followed by the addition of 85% phosphoric acid.

A survey of the literature indicates a number of unexplained and even contradictory data on the properties of optimal VPO catalysts for MA manufacture, especially on the influence of the initial P/V atomic ratio. According to a patent assigned to Chevron (*4*), a maximum of selectivity to MA is reached for P/V ratios in the range $1 < P/V < 2.1$. Hodnett *et al.* (*5*) have observed a distinct rise in selectivity when the P/V ratio is increased from 0.94 to 1.07, while Cavani *et al.* (*6*) reported the opposite effect, i.e., a decrease of MA selectivity on going from 0.95 to 1.16. Debate concerning what phases are present in the best catalysts and especially in the course of the reaction still continues, although most authors agree that

---

[1] To whom correspondence should be addressed.

0021-9517/91 $3.00

$(VO)_2P_2O_7$ (V^{4+}) predominates. A model for the oxidation of butane on the (100) face of this phase was recently proposed (*15*). However, it is generally admitted now that the average oxidation state of vanadium is somewhat greater than 4, suggesting also the participation of vanadium in the 5^+ state, possibly as $VOPO_4$ phases. The activation of the VPO catalysts is another factor which influences the behavior of the final material. The catalyst has been subjected to numerous pretreatments under various inert or reactive atmospheres, and, for each case, the catalytic performance of the final contact mass is different. Optimal activations are obtained by pretreatment with butane/air mixtures (*16–20*). Despite the fact that the most important factors which determine the best catalysts are known, a need of clarification concerning the respective roles of the different crystallographic phases which are formed during the activation and operation of these catalysts exists. (*21*).

An attempt to answer this question, as described in this paper, involves the preparation of two series of VPO catalysts with a fixed preimposed P/V ratio of 1, for which the amount of V^{4+} is controlled at the step of the preparation of the precursor $VOHPO_4$, 0.5 H_2O by adding VCl_3 (V^{3+}) to V_2O_5 (V^{5+}). The catalytic performances of these catalysts were examined in the butane oxidation reaction. The nature and the distribution of the different VPO phases were studied in relation with the catalytic behavior, before and after reaction.

EXPERIMENTAL

1. Catalyst Preparation

The method of preparation of the VPO catalysts is based on the reaction

$$V^{3+} + V^{5+} \rightarrow 2V^{4+}, \qquad (1)$$

where V^{3+} and V^{5+} are introduced as VCl_3 and V_2O_5, respectively. The equilibrium lies largely to the right (equilibrium constant $K \simeq 10^{11}$) so that the V^{3+}/V^{5+} atomic ratio determines the number of V^{4+} ions in the solution.

(*a*) *Preparation in aqueous medium.* A mixture of VCl_3 and V_2O_5 with different V^{3+}/V^{5+} atomic ratios was dissolved in 90 ml of 37% HCl aqueous solution. The dark blue solution obtained was refluxed and stirred for 3 h. The appropriate amount of 85% ortho-H_3PO_4 required to have P/V = 1 was then added to the cooled solution, which was refluxed and stirred for a further 3 h. Excess water was evaporated, and the blue precipitate was dried at 110°C for 24 h.

(*b*) *Preparation in organic medium.* A mixture of VCl_3 and V_2O_5 with different V^{3+}/V^{5+} atomic ratios was suspended in a mixture of 60 ml of isobutyl alcohol and 30 ml of benzyl alcohol. The suspension was stirred continuously under reflux before the amount of 85% ortho-H_3PO_4 required to have P/V = 1 was added. After the phosphoric acid addition, the solution was heated and maintained under reflux with constant stirring for 3 h, the slurry was then filtered, and after washing by isobutyl alcohol, the blue precipitate was dried at 110°C for 24 h.

All catalysts were calcined at 500°C in a flow of nitrogen for 16 h.

On varying the $V^{3+}/V^{5+} = x$ value, with $x = 0.5, 0.75, 1.0$, and 1.5, eight VPO samples were prepared; four samples, denoted $(VPO)_{Aq\,x}$, in aqueous medium and four samples, denoted $(VPO)_{Or\,x}$, in organic medium.

3. Catalyst Characterization

X-ray diffraction patterns were recorded with a Siemens diffractometer using Cu $K\alpha$ radiation.

Specific surface areas of the catalysts were determined by nitrogen adsorption at liquid nitrogen temperature, taking a value of 0.164 nm^2 for the cross section of the adsorbed nitrogen molecule at this temperature.

The valence state of vanadium in the catalysts was determined manganimetrically according to the method of Niwa and Murakami (*22*). The sum of V^{3+} and V^{4+} was determined by direct titration with $KMnO_4$ of the solution containing the dissolved catalyst. The content of total vanadium was determined by titration with iron(II)—ammonium sulfate of the latter solution containing all vanadium as V^{5+}. Similarly, the content of V^{5+} originally present in the catalyst was determined. Through a global balance of the vanadium, it was possible to calculate the separate amounts of V^{3+}, V^{4+}, and V^{5+}.

Infrared spectra were recorded with a Perkin–Elmer 580 spectrophotometer using the KBr disc technique (0.5% dilution).

Diffuse reflectance spectra were obtained with a Perkin–Elmer Lambda 9 spectrophotometer using $BaSO_4$ as a standard.

Raman spectra were recorded on a Dilor Omars 89 spectrophotometer. The emission line at 514.5 nm from Ar^+ laser (Spectra Physics, Model 164) was used for excitation. The output power of the laser source was 16 mW. The sensitivity was adjusted according to the intensity of the Raman scattering. A computer system allowed 100 accumulations for each spectrum. The wave number values obtained from the spectra were accurate to within about 2 cm^{-1}. The assignment of bands was done by comparing the spectra to those of pure VPO phases: α_{II}-, β-, γ-, and δ-$VOPO_4$ and $(VO)_2P_2O_7$.

The NMR ^{31}P examination was performed with a Brucker MSL 300 apparatus using the magic spinning angle method and H_3PO_4 (85%) as standard.

X-ray photoelectron spectroscopy analysis (XPS) was performed with a Hewlett–Packard 5950 interfaced to a data system which allowed the accumulation of spectra. The spectrometer was equipped with an aluminium node ($Al_{K\alpha}$ = 1486.6 eV). All binding energies values were referenced to the C_{1s} line at 284.5 eV. C_{1s}, O_{1s}, V_{2p}, and P_{2p} peaks were recorded.

2. Catalytic Testing

Catalytic tests were carried out in a differential flow microreactor made of Pyrex glass with on-line gas chromatographic analysis; 0.5 g of each catalyst, in the form of powder, was placed in the reactor and heated under nitrogen at 500°C for 1 h. The temperature was then lowered to 370°C and the catalytic activity was measured by flowing 70 ml min^{-1} of a mixture of 2.8% *n*-butane in dry air over the catalyst. For the permanent gases and H_2O, a Delsi IGC 120 MB gas chromatograph equipped with a thermal conductivity detector was used; hydrogen was the carrier gas. Two columns were operated in parallel, a 3-m-$\frac{1}{4}$-in. Molecular Sieve 5A column to separate O_2, CO, and N_2, and a 2-m-$\frac{1}{4}$-in. Porapak Q column to separate CO_2 and H_2O. For the organic products, a Delsi IGC 121 FL gas chromatograph equipped with a flame ionization detector was used; nitrogen was the carrier gas. The column was a 1-m-$\frac{1}{4}$-in. Porapak Q. Butane, maleic anhydride, acetic, and acrylic acids were separated. Catalytic results, butane conversion (C_{But}), and maleic anhydride selectivity (S_{MA}) and yield (ρ_{MA}) were registered at stationary state after stabilization of the activity. Moreover, the stability of all catalysts was verified by measuring the catalytic performances 3 days after the steady state was reached.

RESULTS

The spectra of the precursors of the catalysts prepared in both aqueous and organic media were typical of the $VOHPO_4, 0.5\,H_2O$ phase (*23*), which was the only phase detected. As an example, Fig. 1 gives the spectra for both series for $x = 1.0$. No significant modification of the relative intensities of the (001), (020), and (101) lines was observed and no difference of morphology between all the precursors was evidenced by SEM.

1. Fresh Catalysts

The second row of Table 1 gives the nominal $x = V^{3+}/V^{5+}$ atomic ratio (from VCl_3 and V_2O_5 involved during preparation). The third and fourth rows give the calculated and experimental percentages of V^{4+} (calculated values are based on Eq. (1). A better agreement between the calculated and the experimental results is observed on the $VPO_{\text{Or}x}$ series. It is noticeable that only V^{4+} and V^{5+} were detected and measured, while

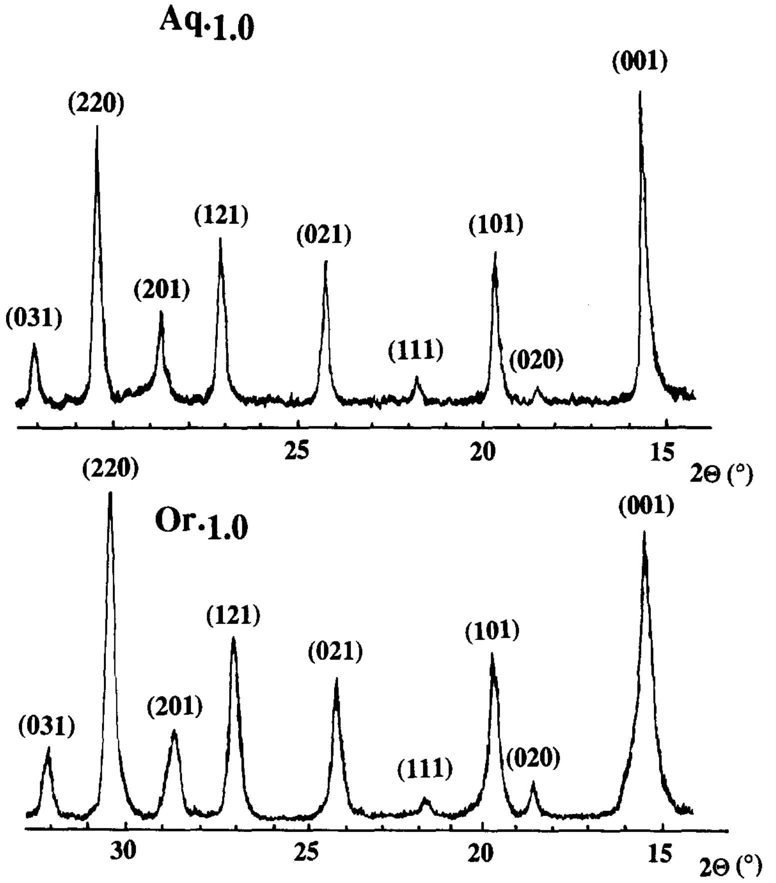

FIG. 1. XRD spectra of two precursors with $x = 1.0$. Aq 1.0, prepared in aqueous medium. Or 1.0, prepared in organic medium.

V^{3+} was not, even for $x = 1.5$, which, according Eq. (1), should contain V^{3+}. It can be observed, from Table 1, that the highest V^{4+} content is observed for $x = 1.0$, simultaneously with a maximum of the BET area for both series of samples.

$(VO)_2P_2O_7$ was the only phase detected by XRD on the fresh catalysts of the $VPO_{Or\,x}$ series, while catalysts appeared to be poorly crystallized for the $VPO_{Aq\,x}$ series.

The infrared spectra shown in Figs. 2 confirmed a crystallinity of the catalysts pre-

TABLE 1

Experimental Data Obtained for Fresh VPO Catalysts

Catalysts:	$VPO_{Aq\,x}$				$VPO_{Or\,x}$			
x:	0.5	0.75	1.0	1.5	0.5	0.75	1.0	1.5
V^{4+}_{calc} (%)	67	86	100	80	67	86	100	80
V^{4+}_{exp} (%)	33	63	96	67	76	84	98	75
S_{BET} (m^2/g)	12.4	20.0	32.0	16.0	19.2	23.0	43.0	21.1

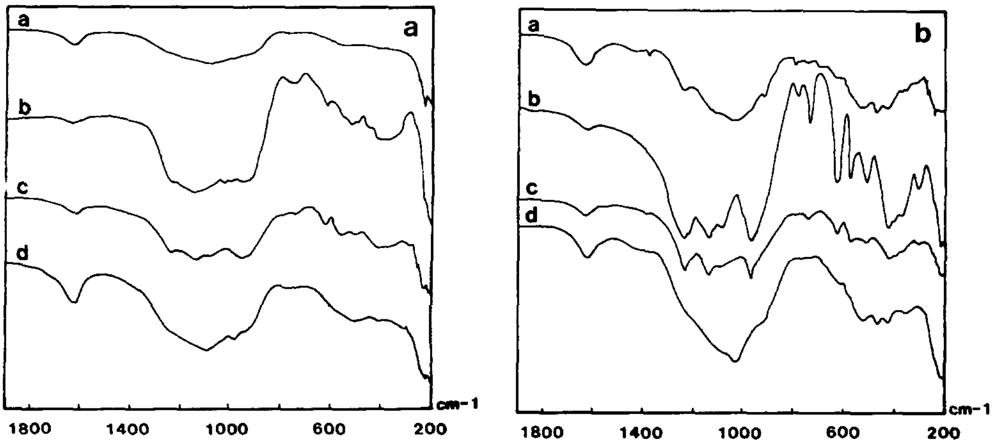

FIG. 2. Infrared spectra (1800–200 cm^{-1}) of fresh catalyst. (a) Prepared in aqueous medium (Aq x) (a, $x = 0.5$; b, $x = 0.75$; c, $x = 1.0$; d, $x = 1.5$). (b) Prepared in organic medium (Or x) (a, $x = 0.5$; b, $x = 0.75$; c, $x = 1.0$; d, $x = 1.5$).

pared in the organic medium better (Fig. 2b) than that of the catalysts prepared in aqueous medium (Fig. 2a). The presence of the pyrophosphate anion characteristic of $(VO)_2P_2O_7$ was evidenced by IR absorption bands observed between 950 and 1250 cm^{-1}, which were assigned to the PO_4 symmetric and antisymmetric stretches (*8*). They are clearly apparent on $VPO_{Or\,0.75}$ and $VPO_{Or\,1.0}$. In contrast, the broad and poorly resolved IR spectra of $VPO_{Aq\,x}$ catalysts predicted the existence of disorganized $(VO)_2P_2O_7$. The broadening of the absorption bands was particularly important for $VPO_{Aq\,0.5}$, which contains a small amount of V^{4+} (33%) (see Table 1).

The diffuse reflectance spectra of fresh catalysts are reported in Figs. 3. Four absorption bands around 300, 500, 650, and 850–900 nm were observed. They are attributed to $(VO)_2P_2O_7$ by comparison with the pure phase (*19*). According to Hanke *et al.* (*28*) and Bordes *et al.* (*8*), the observed bands correspond to $^2A_1 \leftarrow {}^2B_2$, $^2B_1 \leftarrow {}^2B_2$, and $^2E \leftarrow {}^2B_2$ transitions of V^{4+} cations in octahedral symmetry with strong tetrahedral distortion. Moreover, an additional band at 1930 nm and in some cases a small band at 1430 nm were observed. They are attributed to H_2O ($\nu + \delta$) and to H_2O (2ν), respectively. These bands were indicative of some hydration of the catalysts, more pronounced for catalysts prepared in aqueous medium.

2. *Used Catalysts*

Table 2 summarizes some physicochemical and catalytic properties of used VPO catalysts after reaction. Selectivity to MA and conversion of *n*-butane were measured at the steady state, which was attained 4 to 8 h after the beginning of the reaction. The production of MA, which, together with CO_2, was the only product observed, started within the first hour and showed that the catalysts were rapidly activated, in contrast with usual observations for the more conventional catalysts (*4, 20, 30*). The best catalytic results were observed for the $VPO_{Or\,x}$ series. A maximum for conversion and selectivity was reached at $x = 1.0$. $VPO_{Aq\,0.5}$ was particularly inactive for MA formation even after a long period of activation. The catalytic test was accompanied by an important decrease of the surface (compare Tables 1 and 2) and a crystallization of the catalysts, as is evidenced by X-ray diffraction.

2.1. Used catalysts of the aqueous series ($VPO_{Aq\,x}$). Figure 4 presents the XRD spec-

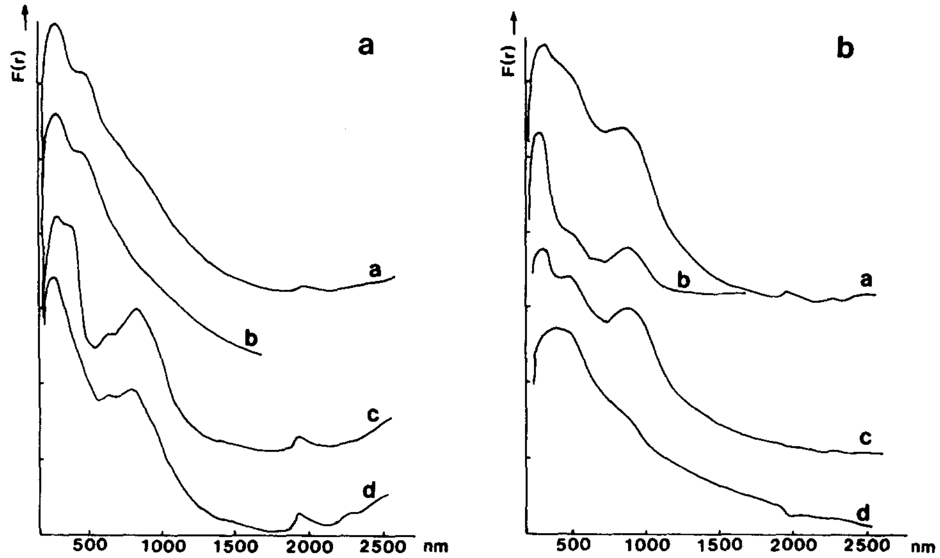

FIG. 3. Diffuse reflectance spectra (2500–300 nm) of fresh catalyst. (a) Prepared in aqueous medium (Aq x) (a, $x = 0.5$; b, $x = 0.75$; c, $x = 1.0$; d, $x = 1.5$). (b) Prepared in organic medium (Or x) (a, $x = 0.5$; b, $x = 0.75$; c, $x = 1.0$; d, $x = 1.5$).

tra of the catalysts after reaction. Crystallisation is relatively high for the $x = 0.75$ and 1.0 samples and very poor for $x = 0.5$ and 1.5. The nature of the crystallographic phases changes with x values, as can be seen in the XRD spectra and as is summarized in the second column of Table 3. Note that, together with $(VO)_2P_2O_7$ and different $VOPO_4$ phases, the importance of the two hydrates $VOH_{0.16}PO_4$, 1.9 H_2O (*A*) (*31*) and $VOPO_4$, $2H_2O$ (*B*), characterized by lines near 12° (2Θ). The presence of these two phases is typical of this series. Their formation occurred during the catalytic test. Indeed our samples were stored after reaction in a dry argon atmosphere, in order to avoid any hydration, which was seen to be possible at room temperature particularly for δ-$VOPO_4$. Table 3 shows the variation of the nature of the VPO phases with x. For $x = 0.5$, the catalyst is poorly crystallized, the hydrates (*A* and *B*) are the principal phases with α_{II}-$VOPO_4$, while $(VO)_2P_2O_7$ appears in a smaller amount. For $x = 0.75$, the quantity of $(VO)_2P_2O_7$ increases, but the hydrates appear to still be the principal phases. Note the presence of β-$VOPO_4$ together with α_{II}-$VOPO_4$. For $x = 1.0$, $(VO)_2P_2O_7$ is the main phase, but the hydrates and the α_{II}-, γ-, and δ-$VOPO_4$ phases are still present. Note that β-$VOPO_4$ is absent in this case. For $x = 1.5$, the catalyst appears to be poorly crystallized and the only phases identified are γ-$VOPO_4$, poorly crystallized $(VO)_2P_2O_7$, and $VOH_{0.16}PO_4$, 1.9 H_2O. A very large broadening of the X-ray lines in the 15–28° (2Θ) domain precludes any identification of other phases.

The Raman technique, which proved to be a very sensitive probe for the presence of $VOPO_4$ entities (*33*), confirmed the higher degree of crystallization for $x = 0.75$ and 1.0 and the lower crystallinity for $x = 0.5$ and especially for the $x = 1.5$ samples. The assignment of phases discussed here (see Table 3) was based on a comparison between the catalysts' spectra and the spectra of the pure phases prepared and analyzed elsewhere (*32*). The Raman spectra are given in the 700–1200 cm^{-1} domain in Fig. 5. By preparing pure $VOH_{0.16}PO_4$, 1.9 H_2O, we have shown that this phase exhibits an

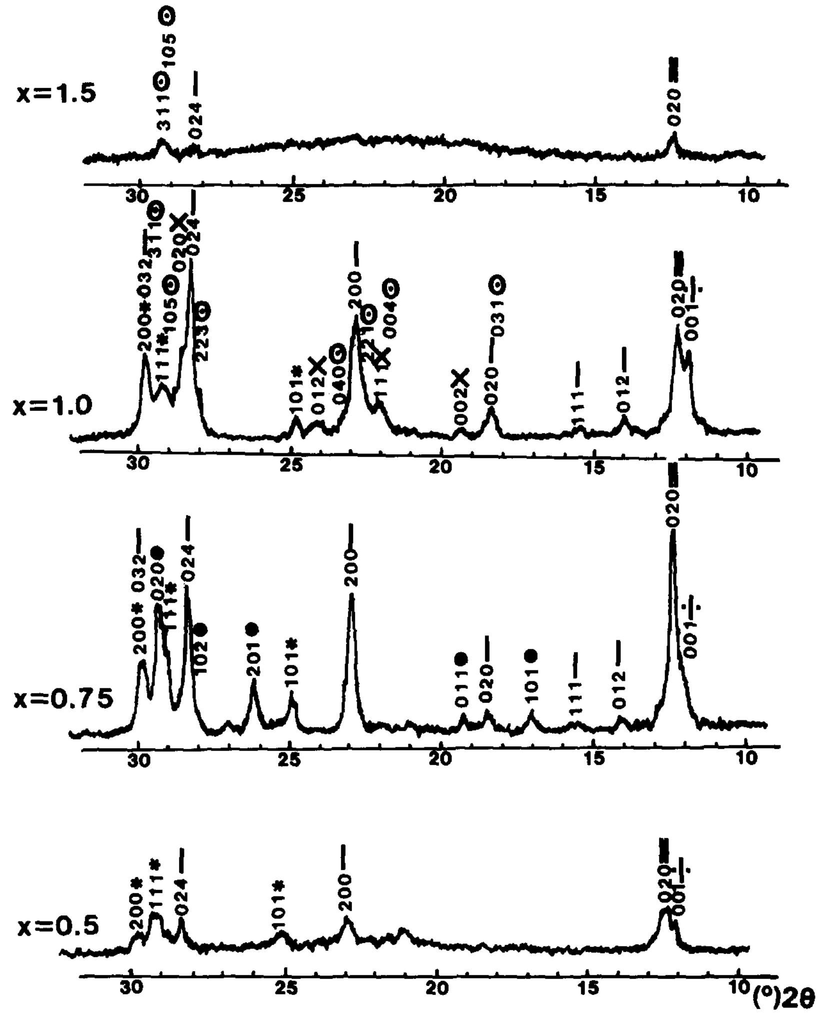

FIG. 4. XRD spectra of used catalysts prepared in aqueous medium (Aq *x*). *, α_{II}-$VOPO_4$; ●, β-$VOPO_4$; ⊙, γ-$VOPO_4$; ×, δ-$VOPO_4$; ‖, $VOH_{0.16}PO_4$, 1.9 H_2O; ·|·, $VOPO_4$, $2H_2O$; |, $(VO)_2P_2O_7$.

TABLE 2

Catalytic Results Obtained at 370°C (2.8% *n*-Butane in Air) with 0.5 g Catalyst and Experimental Data for Used VPO Catalysts

Catalysts:	$VPO_{Aq\,x}$				$VPO_{Or\,x}$			
x:	0.5	0.75	1.0	1.5	0.5	0.75	1.0	1.5
S_{MA} (%)	0	54	93	82	73	66	97	63
C_{BUT} (%)	3	38	41	33	33	47	63	55
ρ_{MA} (%)	0	20	38	27	24	31	61	35
V^{4+}_{exp} (%)	53	60	86	65	73	78	97	80
S_{BET} (m^2/g)	1.1	9.5	17.1	12.5	6.3	15.8	20.5	5.7

TABLE 3

Comparative Discrimination of the Crystalline VPO Phases[a] as Identified by XRD, Raman Spectroscopy, and ^{31}P MAS NMR

x	XRD	Raman spectroscopy	^{31}P MAS NMR
0.5	$VOH_{0.16}PO_4,1.9H_2O$ α_{II}-$VOPO_4$ $(VO)_2P_2O_7$ $VOPO_4,2H_2O$	$(VO)_2P_2O_7$ $VOH_{0.16}PO_4,1.9H_2O$ α_{II}-$VOPO_4$(?)	$(VO)_2P_2O_7$ $VOH_{0.16}PO_4,1.9H_2O$
0.75	$VOH_{0.16}PO_4,1.9H_2O$ $(VO)_2P_2O_7$ β-$VOPO_4$ α_{II}-$VOPO_4$ $VOPO_4,2H_2O$	β-$VOPO_4$ $(VO)_2P_2O_7$ $VOH_{0.16}PO_4,1.9H_2O$ α_{II}-$VOPO_4$(?)	β-$VOPO_4$ $(VO)_2P_2O_7$ $VOH_{0.16}PO_4,1.9H_2O$ α_{II}-$VOPO_4$
1.0	$(VO)_2P_2O_7$ $VOH_{0.16}PO_4,1.9H_2O$ α_{II}-$VOPO_4$ γ-$VOPO_4$ δ-$VOPO_4$ $VOPO_4,2H_2O$	$(VO)_2P_2O_7$ $VOH_{0.16}PO_4,1.9H_2O$ and/or δ-$VOPO_4$ γ-$VOPO_4$ α_{II}-$VOPO_4$	$(VO)_2P_2O_7$ $VOH_{0.16}PO_4,1.9H_2O$ and/or δ-$VOPO_4$ γ-$VOPO_4$ α_{II}-$VOPO_4$ δ/V^{4+}
1.5	γ-$VOPO_4$ $VOH_{0.16}PO_4,1.9H_2O$ $(VO)_2P_2O_7$ (p.c.)[b]	$(VO)_2P_2O_7$ γ-$VOPO_4$ $VOH_{0.16}PO_4,1.9H_2O$ and/or δ-$VOPO_4$	$VOH_{0.16}PO_4,1.9H_2O$ $(VO)_2P_2O_7$ α_{II}-$VOPO_4$ Hydrate/V^{4+}

[a] Phases are classified according to their apparent relative intensities.

[b] p.c., poorly crystallized.

absorption band at 1034 cm^{-1}, at the same frequency as that for δ-$VOPO_4$. α_{II}-$VOPO_4$ can be identified by the band at 992 cm^{-1} only when β-$VOPO_4$ is absent, since the latter has a peak at 997 cm^{-1}. β-$VOPO_4$ is identified by the peak at 893 cm^{-1} (*32*). γ-$VOPO_4$ is identified by the peak at 1020 cm^{-1}. δ-$VOPO_4$ or the hydrates are identified by a peak at 1038 cm^{-1} when γ-$VOPO_4$ is absent, since it absorbs at 1039 cm^{-1}. The lines at 923 and 934 cm^{-1}, which are characteristic of $(VO)_2P_2O_7$, can be superimposed on the intense lines of α_{II}-, γ-, and δ-$VOPO_4$ at 943, 935, and 928 cm^{-1}, respectively, especially when $(VO)_2P_2O_7$ is poorly crystallized. The poor crystallinity of the x = 0.5 and 1.5 samples and the better crystallinity of the 0.75 and 1.5 samples are confirmed. For x = 0.5, the broad band centered at 938 cm^{-1} could be interpreted by the superposition of the 934-cm^{-1} band of $(VO)_2P_2O_7$ on the 943-cm^{-1} band of α_{II}-$VOPO_4$. However, the absence of a band at 992 cm^{-1} makes the identification of α_{II}-$VOPO_4$ questionable by this technique. The band at 1035 cm^{-1} can be attributed to $VOH_{0.16}PO_4$, 1.9 H_2O. For x = 0.75, β-$VOPO_4$ (894, 987, and 1072 cm^{-1}), $(VO)_2P_2O_7$ (927 cm^{-1}), α_{II}-$VOPO_4$ (992 cm^{-1}), and $VOH_{0.16}PO_4$, 1.9 H_2O (1035 cm^{-1}) are identified. For x = 1.0, $(VO)_2P_2O_7$, $VOH_{0.16}PO_4$, 1.9 H_2O, and/or δ-$VOPO_4$ and α_{II}-$VOPO_4$ are detected. Note the absence of β-$VOPO_4$ and the presence of γ-$VOPO_4$ (1019 cm^{-1}). Finally, for x = 1.5, the poor crystallinity makes the assignment more questionable; the presence of $(VO)_2P_2O_7$, γ-$VOPO_4$, and $VOH_{0.16}PO_4$, 1.9 H_2O is however proposed. There is thus very good agreement with the XRD study

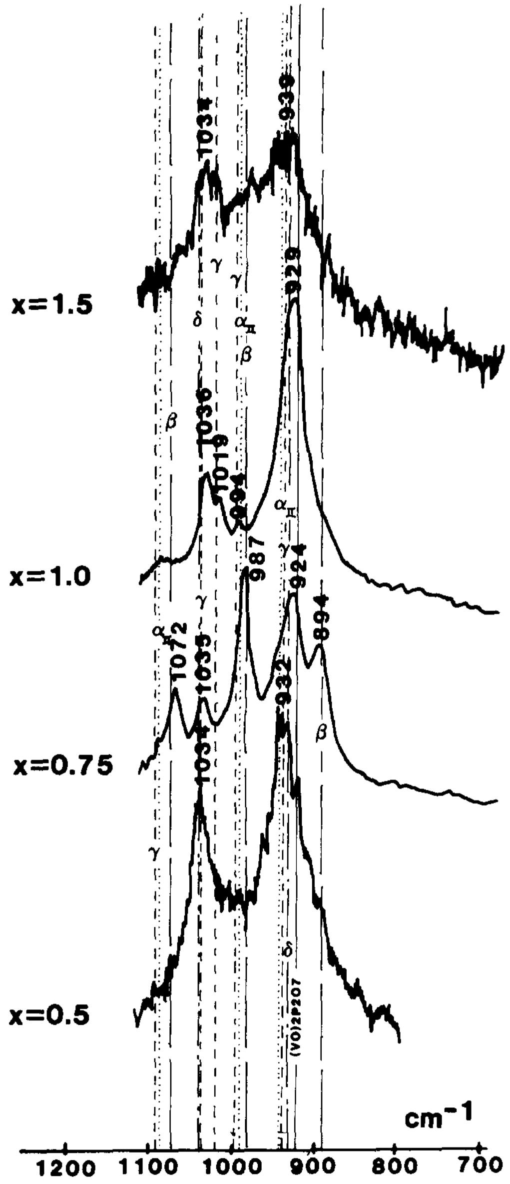

FIG. 5. Raman spectra of used catalysts prepared in aqueous medium (Aq x).

(see Table 3), the Raman spectroscopy being the more specific, owing to its sensitivity to local order, while XRD necessitates longer range order. However, the relative importance of the different phases seems different, since only relative intensities are taken into account.

A ^{31}P MAS NMR study was carried with these catalysts (Fig. 6). According to previous studies (*35*), one can expect a $(VO)_2P_2O_7$ spectrum to exhibit a very braod signal owing to the paramagnetism of V^{4+} (d_1) cations and pure α_{II}-, β-, γ-, and δ-$VOPO_4$ spectra to exhibit a single sharp peak respectively at −19.5, −11.8, −18.8, and +1.6 ppm. The hydrate $VOH_{0.16}PO_4$, 1.9 H_2O, like δ-$VOPO_4$, exhibits a peak at 1.6 ppm with respect to H_3PO_4. Moreover, such peaks may be shifted toward lower frequency with respect to the pure $VOPO_4$ phases, in the case of a high dispersion and a strong interaction of $VOPO_4$ on $(VO)_2P_2O_7$, owing to the paramagnetism of the latter phase. The actual catalysts showed the presence of $(VO)_2P_2O_7$ together with $VOPO_4$ phases (Fig. 6 and Table 3). For all the spectra, $(VO)_2P_2O_7$ was evidenced by a broad and high signal, which was indicative of a high disorganization of the materials and a large dispersion of both V^{4+} and V^{5+} around phosphorus. While only the hydrate (A) was detected with a peak at 2.7 ppm for $x = 0.5$, β-$VOPO_4$ was observed for $x = 0.75$ (−10.3 ppm) with traces of α_{II}-$VOPO_4$ (−19.0 ppm) and the hydrate (A) (2 ppm). $(VO)_2P_2O_7$ was the main phase detected for $x = 1.0$ with a small amount of the hydrate (A) (3.2 ppm) and the γ (−17.4 ppm) and α_{II} (−19.0 ppm) phases. All these phases are not interacting strongly with $(VO)_2P_2O_7$. However, the small peak observed at −11.5 ppm may be attributed to δ-$VOPO_4$ in strong interaction with $(VO)_2P_2O_7$. For $x = 1.50$, the hydrate (A) (3.1 ppm) was the main phase together with $(VO)_2P_2O_7$. The peak observed at −11.2 ppm was tentatively attributed to the hydrate (A) dispersed on $(VO)_2P_2O_7$ and in strong interaction with it.

2.2. Used catalysts of the organic series (*$VPO_{Or\,x}$*). XRD spectra of these samples are presented in Fig. 7 and the detected phases are given in Table 4. For $x = 0.5$ to 1.0, the only phase detected is $(VO)_2P_2O_7$ with the three characteristic (200), (024), and (032) lines at their normal angular positions. Let us consider, however, the shape of the (200) line at 23°, 2Θ. Figure 8 gives an enlarge-

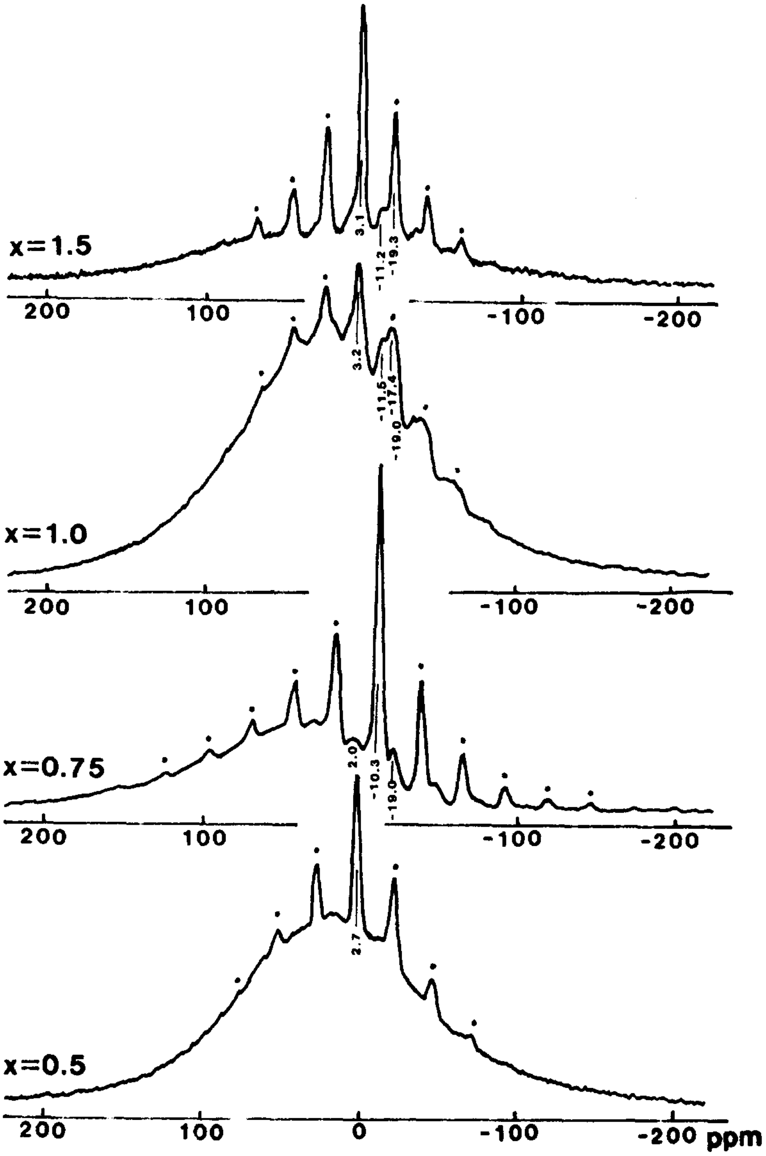

FIG. 6. ^{31}P MAS NMR spectra of used catalysts prepared in aqueous medium (Aq *x*). ●, Participation of rotation bands.

ment of the 20°–25° domain for the three 0.5, 0.75, and 1.0 samples. Around the 23° line position corresponding to the (200) line of $(VO)_2P_2O_7$, we have drawn the two (221) and (040) line positions of γ-$VOPO_4$, at 22.6° and 23.1°, respectively. Looking at this figure, it appears that the broadening of the bottom of the line observed at 23° for the XRD spectrum for $x = 1.0$ can be interpreted by a superposition of these two lines of γ-$VOPO_4$ with the (200) line of $(VO)_2P_2O_7$. As a consequence of this observation, we suggest, aside from $(VO)_2P_2O_7$, the presence of a small amount of γ-$VOPO_4$ in epitaxial growth on $(VO)_2P_2O_7$, visible on the XRD spectrum only at the (221) and (040) positions. The presence of γ-$VOPO_4$ should be ascertained by Raman spectroscopy and by

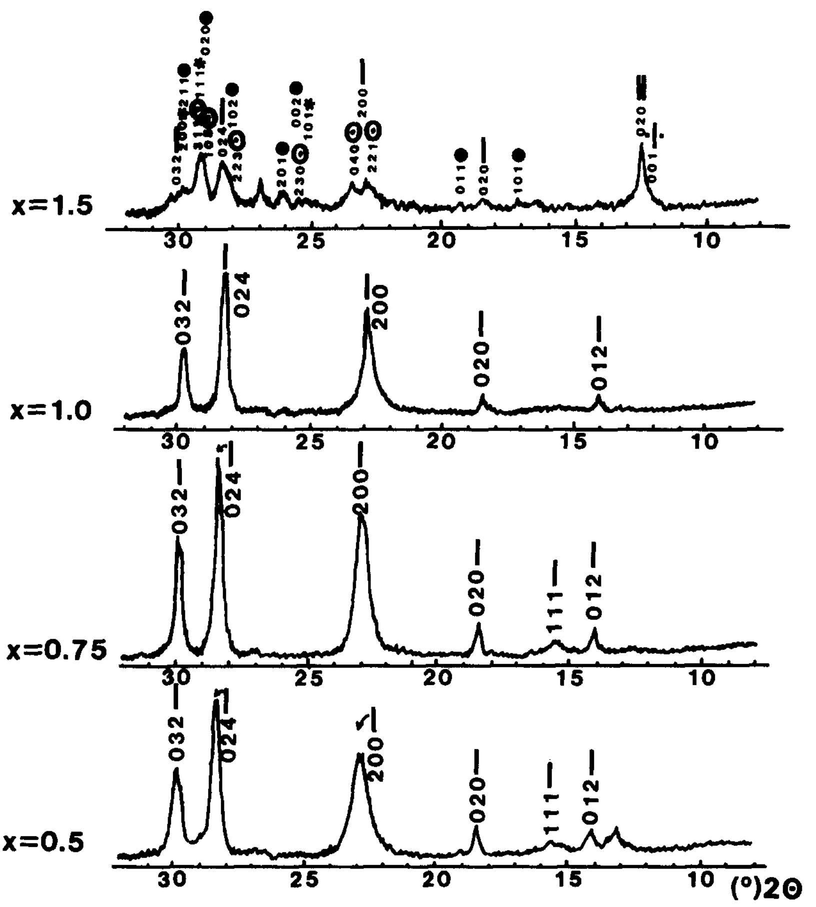

FIG. 7. XRD spectra of used catalysts prepared in organic medium (Or x). *, α_{II}-VOPO$_4$; ●, β-VOPO$_4$; ⊙, γ-VOPO$_4$; ×, δ-VOPO$_4$; ||, VOH$_{0.16}$PO$_4$, 1.9 H$_2$O; ·|·, VOPO$_4$, 2H$_2$O; |, (VO)$_2$P$_2$O$_7$.

^{31}P MAS NMR. We discuss this point below. For $x = 1.5$, all the phases are detected (see Table 4).

Raman spectra are presented in Fig. 9. For all catalysts, the presence of (VO)$_2$P$_2$O$_7$ is confirmed by a band around 930 cm^{-1}. However, we note a progressive displacement of the maximum of this band to higher frequencies by increasing x, which is indicative of the presence of VOPO$_4$ phases. For $x = 0.5$, γ-VOPO$_4$ is observed with a peak at 1020 cm^{-1}. For $x = 0.75$, γ- and δ-VOPO$_4$ can be detected at 1020 and 1037 cm^{-1}, respectively. For $x = 1.0$, a small, broad signal at 1016 cm^{-1} is characteristic of poorly crystallized γ-VOPO$_4$. Finally, for $x = 1.5$, all the phases can be detected with signals at 985 cm^{-1} (α_{II}- and β-VOPO$_4$), 1020 cm^{-1} (γ-VOPO$_4$), 1037 cm^{-1} (γ- or δ-VOPO$_4$, or hydrates), 1070 cm^{-1} (β-VOPO$_4$), 1090 cm^{-1} (α_{II}- and δ-VOPO$_4$), and 920–940 cm^{-1} ((VO)$_2$P$_2$O$_7$ and α_{II}-, γ-, and δ-VOPO$_4$). These results are in agreement with those from XRD (see Table 4).

^{31}P MAS NMR spectra are given in Fig. 10. For $x = 0.5$ and 1.0, the absence of any narrow peaks shows that bulk VOPO$_4$ phases are absent, in agreement with the XRD observations. The absence of a broad signal as observed for samples prepared in aqueous medium can be interpreted by a better organization of the whole system, which appears to be a characteristic of these catalysts. The presence of crystallized VOPO$_4$ phases is observed for $x = 0.75$ with γ-VOPO$_4$ (-18.8 ppm) and δ-VOPO$_4$ or hy-

TABLE 4

Comparative Discrimination of the Crystalline VPO Phases[a] Prepared in Organic Medium (Or x) as Identified by XRD, Raman Spectroscopy, and ^{31}P MAS NMR

x	XRD	Raman spectroscopy	^{31}P MAS NMR
0.5	$(VO)_2P_2O_7$	$(VO)_2P_2O_7$ γ-$VOPO_4$	$(VO)_2P_2O_7$ $VOH_{0.16}PO_4$,1.9H_2O and/or δ-$VOPO_4$ (tr)[b]
0.75	$(VO)_2P_2O_7$ γ-$VOPO_4$ (?)	$(VO)_2P_2O_7$ γ-$VOPO_4$, δ-$VOPO_4$	$(VO)_2P_2O_7$ $VOH_{0.16}PO_4$,1.9H_2O and/or δ-$VOPO_4$ γ-$VOPO_4$
1.0	$(VO)_2P_2O_7$ γ-$VOPO_4$	$(VO)_2P_2O_7$ γ-$VOPO_4$	$(VO)_2P_2O_7$ γ-$VOPO_4$
1.5	β-$VOPO_4$ $(VO)_2P_2O_7$ γ-$VOPO_4$ α_{II}-$VOPO_4$ $VOH_{0.16}PO_4$,1.9H_2O $VOPO_4$,2H_2O	$(VO)_2P_2O_7$ $VOH_{0.16}PO_4$,1.9H_2O β-$VOPO_4$ α_{II}-$VOPO_4$ (?) γ-$VOPO_4$	β-$VOPO_4$ $(VO)_2P_2O_7$ γ-$VOPO_4$ $VOH_{0.16}PO_4$,1.9H_2O and/or δ-$VOPO_4$

[a] Phases are classified according to their relative intensities.
[b] tr, as traces.

drate (2.7 ppm) and for $x = 1.5$ with β-$VOPO_4$ (-10.8 ppm) and trace amounts of γ-$VOPO_4$ (-20.8 ppm) and δ-$VOPO_4$ or hydrate (2.1 ppm) (see Table 4). The agreement with the two previous techniques appears to be very good.

3. *Superficial Properties as Determined by XPS*

Several samples have been analyzed before or after butane oxidation reaction was carried out and without any further treatment in the spectrometer. The experimental data are summarized in Table 5. The main features may be summarized as follows:

i. Binding energy values of V_{2_p} peaks at 517 and 524.5 eV for $2p^{3/2}$ and $2p^{1/2}$, respectively, are identical for all samples. Such values may correspond to $(VO)_2P_2O_7$ by comparison with literature data (*40*). Recall that binding energy values are increasing with the ionic character of the V–O bond (*41*).

ii. A second peak at 518 eV for $V_{2p^{3/2}}$ was also observed for samples prepared in aqueous medium, after reaction. By comparison with XRD data, it can be suggested that it corresponds to $VOPO_4$ species.

iii. A strong shoulder in the O_{1s} peak at +1 eV binding energy value was observed after catalysis for both aqueous medium samples analyzed ($x = 0.5$ and 1.5). By comparison with XRD data, it may be suggested that it corresponds to hydrated $VOPO_4$.

iv. The measured atomic ratios (V/O, P/O, and P/V) do not correspond to those obtained by chemical analysis. This clearly indicates that the surface layer is poor in V and rich in P. Such a feature has been mentioned by several authors (e.g., (*40, 42*)) and was suggested to induce an increase in surface acidity (*40*). Such an excess is observed (compare Tables 2 and 5) to be unfavorable when it is too large (>2.3 for aqueous medium samples).

DISCUSSION OF RESULTS

The preparation of VPO catalysts in both organic and aqueous media by controlling the amount of V^{4+} from $V^{3+} + V^{5+}$ redox

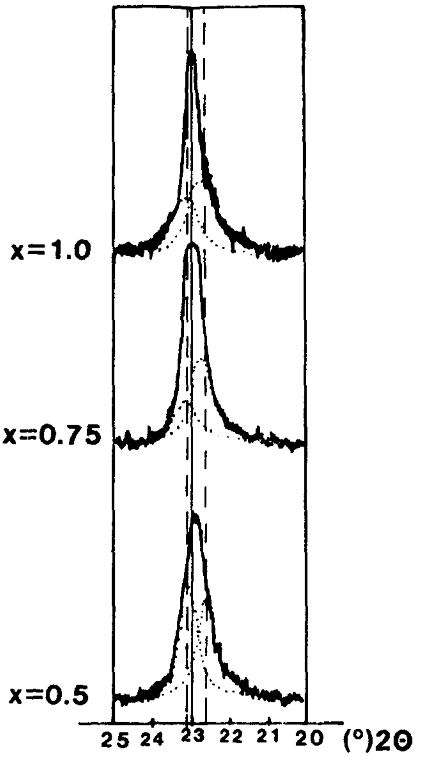

FIG. 8. Broadening of the 20–25° 2Θ domain for the XRD spectra of the $VPO_{Or,x}$ catalysts (x = 0.5, 0.75, and 1.0).

reaction is an alternative way of synthesizing good catalysts for the selective oxidation of *n*-butane to maleic anhydride. By varying the initial $x = V^{3+}/V^{5+}$ ratio between 0.5 and 1.5, it was shown that it was possible to stabilize V^{4+} cations in the final VPO catalysts. The best agreements between the amounts of V^{4+} predicted by the redox $V^{3+} + V^{5+} \rightarrow 2V^{4+}$ reaction and the amount of V^{4+} as determined by chemical analysis were obtained for values of x = 1.0 and for reaction conducted in an organic medium. This original method led to catalysts having different textures (specific surface area) and compositions (nature of the different $VOPO_4$ phases present with $(VO)_2P_2O_7$). As a consequence, a strong influence was observed on the catalytic properties, both on the butane conversion and on the selectivity to maleic anhydride (controlled by the nature of the different phases and their relative organization).

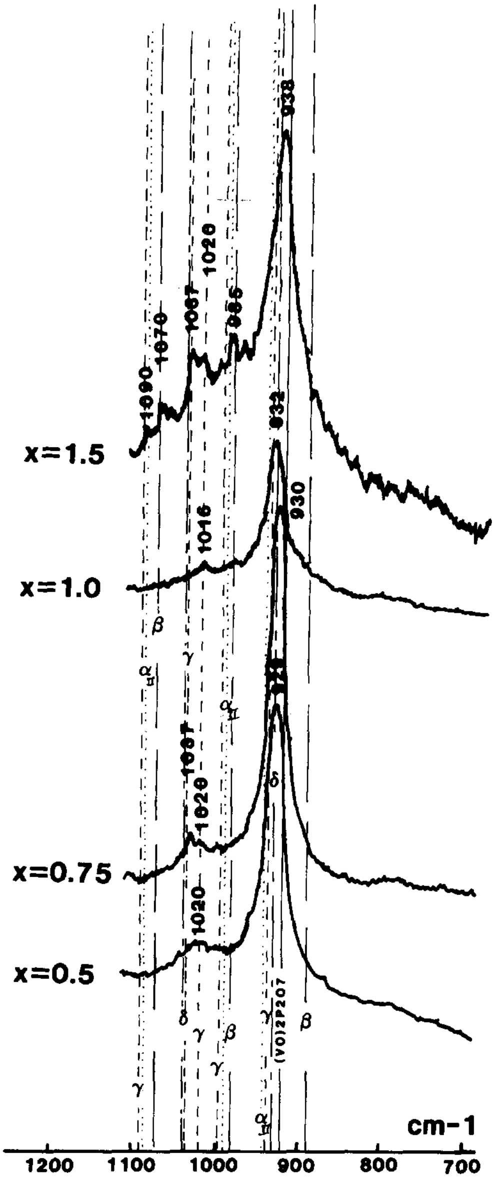

FIG. 9. Raman spectra of used catalysts prepared in organic medium (Or x).

The study by different techniques, like XRD, Raman spectroscopy, MAS NMR, and XPS, which are not sensitive to the same physicochemical characteristics of the catalysts enabled us to obtain new information on the important features of VPO catalysts for the mild oxidation of butane to maleic anhydride. Indeed, consideration of Tables 3 and 4 shows that there is a very

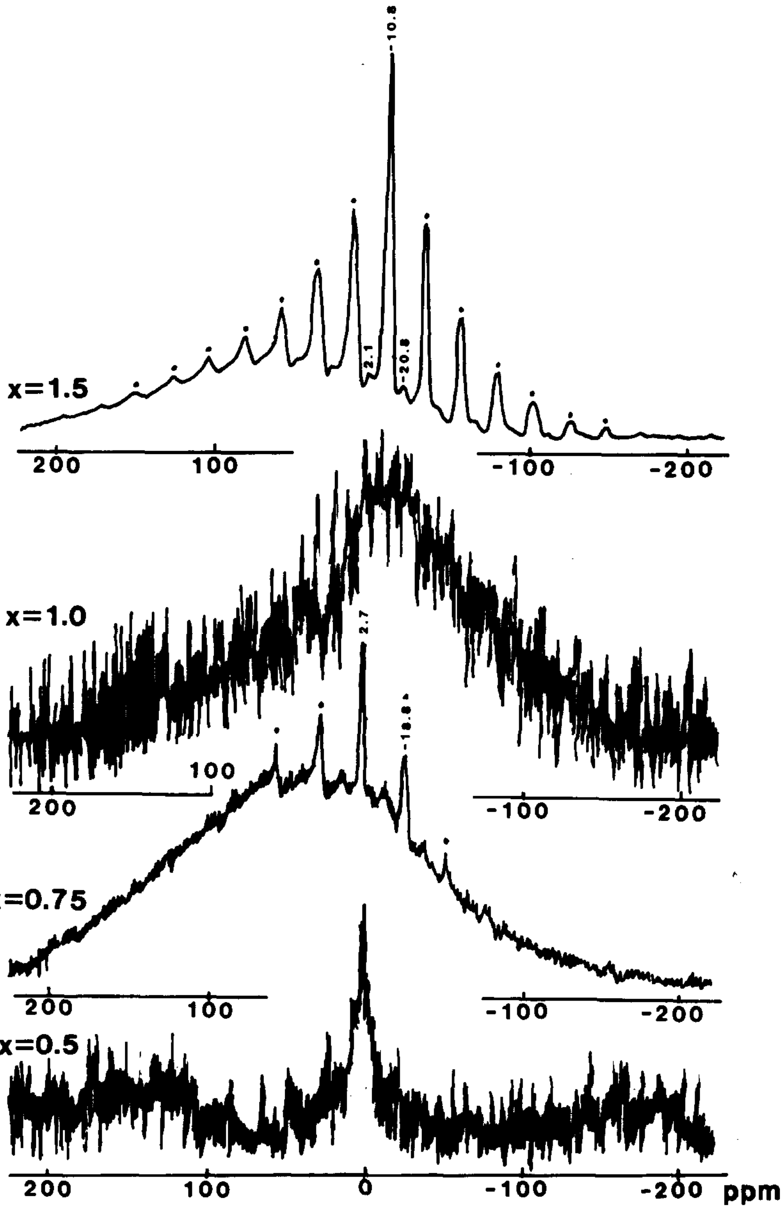

FIG. 10. ^{31}P MAS NMR spectra of used catalysts prepared in organic medium (Or x). ●, Participation of rotation bands.

good agreement between XRD, Raman spectroscopy, and ^{31}P MAS NMR studies concerning the identification of the different crystalline phases in the catalysts. Consequently, the confrontation with the catalytic results given in Table 2 led us to propose the following conclusions:

1. The best catalytic results for MA formation are observed when $(VO)_2P_2O_7$ is the principal phase in the catalyst (see $VPO_{Or\ 1.0}$). However, high selectivity to MA is also observed when specific $VOPO_4$ phases are simultaneously present (see $VPO_{Aq\ 1.0}$ and $VPO_{Aq\ 1.5}$). These conclusions are in agreement with the measured V^{4+} content.

2. Good selectivities to MA appear to be related to the presence of γ-$VOPO_4$ associated with $(VO)_2P_2O_7$. This conclusion can be

TABLE 5

XPS Data Obtained for Some Aqueous and Organic Media Samples Before (*A*) and After (*B*) 8 h of Catalytic Reaction

Samples	$VPO_{Or\ 1.0}$		$VPO_{Aq\ 0.5}$		$VPO_{Aq\ 1.5}$
	A	B	A	B	B
Binding energy values[a] (eV)					
P_{2p}	133.6	133.6	133.8	133.5	133.8
O_{1s}	531.3	531.35	531.6	531.2[b]	531.4[b]
V_{2p}	516.9	517	517	517[c]	517
	−524.5	−524.5	−524.5	−524.7	−524.7
Atomic ratios[d]					
V/O	0.143	0.135	0.077	0.103	0.09
P/O	0.235	0.235	0.203	0.236	0.25
P/V	1.64	1.73	2.65	2.3	2.85

[a] Values referenced to C_{1s} = 284.5 eV to compensate for a charging effect which was rather small (<0.3 eV). Values given ±0.2 eV.

[b] A shoulder was observed at +1 eV binding energy value.

[c] A second peak was detected at +1 eV binding energy value, presumably corresponding to V^{5+} cations.

[d] Calculated using the approximate relationship

$$n_1/n_2 = I_1 \cdot \sigma_2 \sqrt{E_{k2}}/I_2 \cdot \sigma_1 \sqrt{E_{k1}}.$$

drawn from the two series of samples (see $VPO_{Aq\,1.0}$, $VPO_{Aq\,1.5}$, and all the $VPO_{Or\,x}$ catalysts).

3. The highest yields to MA (61%) for $VPO_{Or\ 1.0}$ are observed when γ-$VOPO_4$ is associated with $(VO)_2P_2O_7$ on an organized matrix.

4. The role of the other $VOPO_4$ phases in association with $(VO)_2P_2O_7$ can also be discussed. The presence of α_{II}-$VOPO_4$ leads to poor results ($VPO_{Aq\ 0.5}$) as does β-$VOPO_4$($VPO_{Aq\,0.75}$ and $VPO_{Or\,1.5}$). It is more difficult to discriminate the role of δ-$VOPO_4$ in so far as it cannot be separated from that of the two hydrates. (The same signals are observed by Raman spectroscopy and by MAS NMR).

This work led us to conclude that $(VO)_2P_2O_7$ is not the unique VPO phase responsible for the oxidation of butane to maleic anhydride as proposed recently. The mean oxidation state of 4.1 currently measured by many authors on classical VPO catalysts prepared in organic medium from V_2O_5, H_3PO_4, and isobutanol was in favor of the participation of some $VOPO_4$ species in the mechanism of oxidation of butane with $(VO)_2P_2O_7$. Our results confirm the role played by these $VOPO_4$ species. The higher P/V superficial ratio observed by XPS lead us to think that, owing to their acidity, the PO_4 groups on the surface of $(VO)_2P_2O_7$ should be responsible for the activation of the C–H bond of butane and thus should control the first step of the mechanism. An optimal superficial P/V ratio (1.7) seems to be necessary. Further steps involving the O insertion could be controlled by the presence of $VOPO_4$ entities like γ-$VOPO_4$. We are of the opinion that the actual catalyst consists of such γ-$VOPO_4$ islands on a $(VO)_2P_2O_7$ matrix, probably in epitaxial growth, as suggested by XRD and ^{31}P MAS NMR. As a consequence, the catalytic results should be controlled by the interfaces between these two phases.

ACKNOWLEDGMENTS

The authors are indebted to Dr. R. Olier and to Dr. F. Lefebvre for the Raman spectroscopy and MAS

NMR measurements, respectively. They thank Dr. G. Coudurier, R. Olier, F. Lefebvre, and R. P. A. Sneeden for fruitful discussions.

REFERENCES

1. Hucknal, D. J., "Selective Oxidation of Hydrocarbons." Academic Press., Londres, 1974.
2. Hodnett, B. K., *Catal. Rev. Sci. Eng.* **27**(3), 373 (1985).
3. Varna, R. L., and Saraf. D. M., *Ind. Eng. Prod. Res. Dev.* **18,** 7 (1975).
4. Schneider (to Chevron Research Co.), U.S. Patent 3,864,280, 1975.
5. Hodnett, B. K., Permanne, P., and Delmon, B., *Appl. Catal.* **6,** 231 (1983).
6. Cavani, F., Centi, G., and Trifiro, F., *Appl. Catal.* **9,** 191 (1984); *J. Chem. Comm.*, 492 (1985).
7. David, M., Thesis, Lyon, 1988.
8. Bordes, E., and Courtine, P., *J. Catal.* **57,** 236 (1979).
9. Jordan, B., and Calvo, C., *Canad. J. Chem.* **51,** 2621 (1973).
10. Kasumoto, K., and Marquis, D. M., U.S. Patent 4,132,670 1979.
11. Nakamura, M., Kawai, K., and Fujiwara, Y., *J. Catal.* **34,** 345 (1974).
12. Martine, G., Morselli, L., Riva, A., and Trifiro, F., *React. Kinet. Catal. Lett.* **8,** 431 (1978).
13. Poli, G., Ruggeri, O., and Trifiro, F., "Proceedings, 9th International Symposium on React. of Solids, Cracow, 1980," p. 512.
14. U.S. Patent 4,562,268, 1981.
15. Ziolkowski, J., Bordes, E., and Courtine, P., *J. Catal.* **122**(1), 126 (1990).
16. Hodnett, B. K., and Delmon, B., *Ind. Eng. Chem. Fundam.* **23,** 4665 (1984).
17. Pyatnitskaya, A. I., Komasko, G. A., Zazhigalov, V. A., and Gorokhovatskii, B. B., *React. Kinet. Catal. Lett.* **6,** 341 (1977).
18. Freerks, M. C., and Mount, R. A., U.S. Patent 3,977,988, 1976.
19. U.S. Patent 3,864,280, 1975.
20. Hutchings, R. J., and Higgins, R., U.S. Patent 4,288,372, 1981.
21. Bordes, E., *Catal. Today* **1**(5), 499 (1987).
22. Niwa, M., and Murakami, Y., *J. Catal.* **76,** 9 (1982).
23. Johnson, J. W., Johnston, D. C., Jacobson, A. J., and Brody, J. F., *J. Amer. Chem. Soc.* **106,** 8123 (1984).
24. Hezel, A., and Ross, S. D., *Spectrochim. Acta* **24A,** 131 (1968).
25. Cordridge, D. E., and Lowe, E. J., *J. Chem. Soc.*, 493, (1954).
26. Chapman, A. C., and Thirwell, L. E., *Spectrochim. Acta* **20,** 937 (1964).
27. Ballhausen, C. J., and Gray, H. B., *Inorg. Chem.* **1,** 111 (1962).
28. Hanke, W., Biernert, R., and Ezrschkewitz, H. G., *Z. Anorg. Allg. Chem.* **414,** 109 (1975).
29. King, E. F., and Good, M. L., *Spetrochim. Acta* **29,** 707 (1973).
30. Buchanan, J. S., Apostolakis, J., and Sundersan, S., *Appl. Catal.* **19,** 65 (1985).
31. Schneider, A. Thesis, Bordeaux, 1987.
32. Ben Abdelhouahhab, F., Guilhaume, N., Olier, R., and Volta, J. C., submitted for publication.
33. Moser, T. P., and Schrader, G. L., *J. Catal.* **92,** 216 (1985).
34. Vedrine, J., Milklet, J. M., and Volta J. C., *Faraday Discuss. Chem. Soc.* **87,** 1 (1989).
35. David, M., Lefebvre, F., and Volta, J. C., "Proceedings, 11th Ibero American Symposium on Catalysis, Guanajuarato, Mexico, 1988," p. 365.
36. Moser, T. P., and Schrader, G. L., *J. Catal.* **104,** 99 (1987).
37. Garbassi, F., Bart, J. C. J., Montino, F., and Petrini, G., *Appl. Catal.* **16,** 271 (1985).
38. Bordes, E., Courtine, P., and Johnson, J. W., *J. Solid State Chem.* **55,** 270 (1984).
39. Bordes, E., Johnson, J. W., Raminosona, A., and Courtine, P., "Proceedings, 10th International Symposium on Reactivity of Solids, Dijon, 1984," p. 502.
40. Zazhigalov, V. A., Belousov, V. M., Komashko, G. A., Pyatnitskaya, A. I., Merkureva, Y. N., Poznyakevich, A. L., Stoch, J., and Haber J., *in* "Proceedings, 9th International Congress on Catalysis, Calgary, 1988" (M. J. Phillips and M. Ternan, Eds.), p. 1546. Chem. Institute of Canada, Ottawa, 1988.
41. Siew Hew Sam, D., Soenen, V., and Volta, J. C., *J. Catal.* **123,** 417 (1990).
42. Haas J., Plog, C., Maunz W., Mittag, K., Gollmer, K. D., and Klopries B., *in* "Proceedings, 9th International Congress on Catalysis, Calgary, 1988" (M. J. Phillips and M. Ternan, Eds.), p. 1632. Chem. Institute of Canada, Ottawa, 1988.